International Journal of Mechanical Production
Engineering Research and Development (IJMPERD)
ISSN(P): 2249-6890; ISSN(E): 2249-8001
Vol. 4, Issue 4, Aug 2014, 23-36

EFFECT OF HEAT-FLUX BOUNDARY ON BUOYANCY-DRIVEN FLOW IN A TWO-DIMENSIONAL SQUARE-ENCLOSURE UTILIZING Cu-H_2O NANO-FLUID

SIDDHARTHA KOSTI

Department of Mechanical, Indian Institute of Technology Kanpur, Uttar Pradesh, India

ABSTRACT

A numerical investigation of buoyancy-driven flow in a two-dimensional square enclosure filled with Cu-H_2O nanofluid has been studied. On one wall heat flux boundary and on the other three walls convective boundary conditions have been conducted. Different pertinent parameters of the present study are Grashof number (5×10^5) and solid nanoparticle concentration ϕ (varying up to 8%) and inclination angles λ. Prandtl number for water has been kept to a constant value of (Pr =6.49). Results shows that fluid flow is very sensitive to the inclination angles values, mild conduction has been observed when heat flux is at the top wall, while an extra rolls at the bottom corner of the enclosure has been found for 37° inclination angle. Addition of nano-particle in the base-fluid is not showing any changes in the flow patterns and temperature and velocity profiles. Nusselt number is also found to be decreasing with particle concentration values.

KEYWORDS: Convective Boundary, Heat Flux Boundary, Nanofluid, Particle Concentration and Enclosure

INTRODUCTION

Natural convection in an enclosure has been extensively studied by many researchers because of its many different applications. One of the most studied problems is enclosure with two horizontally insulated walls and two vertical isothermally heated walls at different temperatures or two vertically insulated walls and two horizontally isothermal walls which is also known as Rayleigh-Benard convection type problem. Now a day's nanofluid has attracted the attention of the researchers around the globe because compared to conventional fluids like water, oil and ethylene glycol mixture, nano-fluids have good thermal properties like high thermal conductivity, higher heat transfer coefficient [1], higher surface area to volume ratio (1000-times) and reduced particle clogging as compared to millimetric size particles etc. In present study cupper has been used as a solid nanoparticle because of its higher thermal conductivity value. Water has been used as a base fluid. Colloidal suspension of solid nanoparticle in the base fluid called nanofluid. Nanofluid has been completely restrained inside the enclosure and it flows because of the temperature differences between the walls. Present study here deals with numerical simulation of natural convection in an enclosure. On the left wall of the enclosure constant heat flux boundary condition has been implemented while all the other three walls are losing heat to the surrounding by convection.

Due to its wide applications simple geometry natural convection inside an enclosure has been studied by many researchers. Khanafer et al. [2] in 2003 numerically studied the effect of cu-water nano-fluids considering dispersion effect on buoyancy-driven flow in two-dimensional square enclosure and noticed that nano-particles in the base fluid enhances the heat transfer rate and it increases with increment in particle concentration. They found that dispersion effect increases

with increase in particle concentration. Abu-Nada and Oztop [3] in 2009 numerically studied the effect of inclination angle on natural convection in square enclosure filled with Cu-H_2O nanofluid. They found that flow pattern does not get affected by the particle concentration at 90° inclination angle and also found lowest heat-transfer enhancement at this angle. At low values of Rayleigh number inclination angle does not affect heat-transfer enhancement rate. Rubel and Landis [4] in 1969 numerically studied the natural convection in two-dimensional rectangular enclosure for different Rayleigh number and prandtl number for an aspect ratio of 5.0 and found that cell gets strengthen with increasing Ra value and found maximum at $Ra=2.4\times10^5$. Flow pattern found to be strongly depends on the prandtl number for low values less than 1.0 but higher values does not influences flow pattern.

Hiroyuki et al [5] in 1974 experimentally and numerically studied the natural convection in an inclined enclosure. They noticed maximum heat transfer rate at an inclination angle around 50° from the horizontal plane both numerically and experimentally. A minimum heat transfer rate has been found by them when hot and cold surfaces are inclined at an angle of 10° from the horizontal plane. Ghasemi and Aminosaadati [6] in 2009 numerically studied the natural convection heat transfer in an inclined enclosure filled with CuO-H_2O nano-fluid. They found maximum average Nusselt number for an optimum value of inclination angle. Different flow pattern at high Rayleigh number for zero degree inclination angle compare to other inclination angles while same flow patterns have been found by them at low Rayleigh number between 30° and 90° inclination angle. Ogut [7] in 2009 numerically studied the natural convection of water-based nano-fluids in an inclined enclosure with a heat source at left vertical wall. He noticed that length of the heater at left vertical wall affect the heat transfer enhancement. He also found that average heat transfer rate decreases with increasing heater length for small inclination angle and noticed maximum heat transfer at 30° while minimum heat transfer occurs at 90°.

Santra et al [8] in 2008 numerically studied the heat transfer augmentation in a differentially heated square cavity using Cu-H_2O nanofluid. They found that with increment in solid particle volume fraction for any Rayleigh number considered heat transfer decreases. They found no heat transfer increment for low Ra values. They also found that heat transfer increases with increase in Rayleigh number. Rong-Yuan and Tzeng [9] in 2006 numerically studied the natural convection heat transfer enhancement filled with nano-fluids in rectangular enclosure. They found that enhancement is very sensitive for nanofluids compared to base-fluids. They noticed an increase in average Nusselt number and flow rates with Rayleigh number. They also noticed increment in Nusselt number with decrement in aspect ratio. Alloui, Z. et al [10] in 2012 analytically and numerically studied the buoyancy-driven convection in a vertical enclosure filled with nano-fluids. They considered three different nano-particles Cu, Al_2O_3 and TiO_2. They developed two heat transfer equation in the form of Nusselt number for two different regime based on parallel flow approximation analytically. They had used different model for kinematic viscosity and found that it affects the heat transfer performance of the nanofluid by a considerable amount. They also observed that Cu gives higher heat transfer enhancement compared to other nano-particle because of its higher thermal conductivity value.

Das and Tiwari[11] in 2007, Talebi et al [12] in 2010 and Khanafer et al [13] in 2007 numerically studied the mixed convection in a lid-driven cavity. Das and Tiwari and Talebi et al utilize Cu-H_2O nano-fluid and found that average Nusselt number increases with solid particle concentration while Khanafer et al. used pure-fluid and oscillating sinusoidal lid-driven and noticed that average Nusselt number increases with Grashof number and decreases with Reynolds number and lid frequency increment. Jang et al [14] in 2004 studied the role of Brownian motion in the enhancement in thermal conductivity of the nano-fluids. They observed four modes of energy transport in the nano-fluids: Due to collision between

base fluid materials, thermal diffusion of nanoparticles in the base fluid, collision between nanoparticle molecules and collision between nanoparticle and base fluid molecules. They observed that effect of third mode is very less compare to other three modes on enhanced thermal conductivity. They noticed that as the particle size decreased or temperature increased random motion increased, due to which convection effect becomes dominant which increases the effective thermal conductivity.

Azizian et al [15]in 2009 studied the effect of nanoconvection due to Brownian motion on thermal conductivity of nano-fluids. They concluded that enhancement in heat transfer can be due to four reasons Interfacial layer, Brownian motion, nanoparticle clustering, and nature of heat transport in nanoparticles. They compare three different time scale due to nanoconvection diffusion, heat diffusion, Brownian motion diffusion and concluded that movement of nanoparticle due to Brownian motion is too slow compare to heat diffusion and also noticed that nanoconvection diffusion is comparable to heat diffusion. Finally they concluded that the Brownian motion effect is important in thermal transport. Brinkman [16] in 1952 studied the viscosity of concentrated suspension and solution. He developed a model for the effective dynamic viscosity of solution or suspensions of finite concentration. The model has included concentration effect in it.

Murshed et al [17] in 2011 studied the contribution of Brownian motion in thermal conductivity of nano-fluids. They developed a new model for effective thermal conductivity considering both static and dynamic mechanisms. In their model they considered the effect of particle size, Brownian motion, fluid temperature, interfacial layer. They concluded that as the particle size decreases randomness increases and effective thermal conductivity increases. They concluded that contribution due to dynamic mechanism are not applicable for $\phi<0.002$. They compare their results for three nanoparticle TiO_2, CuO and Al_2O_3 with the experimental results available in the study and found in good agreement.

Singh [18] in 2008 studied the thermal conductivity of nano-fluids: review paper. He concluded that nano-fluids have some good properties compare to base fluid, increase thermal conductivity, increase single phase heat transfer coefficient and increase critical heat flux. He told that there are two types of model for nanofluid, one is static model in which nanofluid assumes stationary in the base fluid second one is dynamic model due to transport or random movement of nanoparticles enhances heat transfer due to collision. They dictated numerous applications where nano-fluids can be used like in Bio-medical, space applications, automobile fields, military applications, coolants etc.

From above literature review one can notice that combination of constant heat flux and convective boundary condition has not been studied in detail so it a subject of great study. So the aim of present study is to see the effect of different boundary condition on the fluid flow patterns and heat transfer. The present study here deals with numerical simulation of laminar incompressible buoyancy driven flow in a two-dimensional square enclosure utilizing Cu-H_2O of nano-fluid. Left wall has been subjected to constant heat flux boundary condition while from other three walls heat is losing to the surrounding by convection. Main aim of this study is to see the effect of different parameters on heat transfer enhancement. Considering the amount of heat flux q" to be $1000W/m^2$ a Grashof number has been calculated to 5×10^5. Cupper Nano-fluids has been considered in the study to see the effect of different thermal properties compared to base fluid as shown in Table 1, solid particle concentration of these nano-particles is varying from ϕ (0 - 8%). Nu_{air} which is coming due to convective boundary condition has been calculated based on the h_{air}, k_{air} (heat transfer coefficient and thermal conductivity of air respectively) value.

NOMENCLATURE

C_p	Specific Heat	**Greek Symbol**	
G	Gravitational acceleration	α	Thermal Diffusivity
H	Heat Transfer Coefficient	β	Thermal Expansion Coefficient
x, y	Cartesian co-ordinates	ω	Vorticity
H	Height of Enclosure	μ	Dynamic Viscosity
L	Length of Enclosure	ν	Kinematic Viscosity
K	Thermal Conductivity	ψ	Stream function
$q^{"}$	Heat Flux	ρ	Density
T	Time	θ	Non-dimensional Temperature
T	Temperature	λ	Inclination angle
ΔT	Temperature difference	ϕ	Nano-particle concentration
U	Horizontal velocity component	**Subscript**	
V	Vertical velocity component	f	Base-fluid
AR	Aspect Ratio	nf	Nano-fluid
Gr	Grashof Number	s	Solid-particle
Pr	Prandtl Number	∞	Ambient
Nu	Nusselt Number	Ref	Reference value

MATHEMATICAL FORMULATION

Problem Statement

Schematic of square enclosure has been shown in Figure 1. As one can notice that heat flux boundary condition has been considered on the top wall of the enclosure while on other three walls convective boundary condition has been considered. Convective boundary condition states that heat is losing to the surrounding by free convection. The mixture of Cu-H_2O nano-particle and base-fluid which is water is assumed to be in single phase. No-slip conditions between the nano-particle and water particle is considered and both are also assumed to be in thermal equilibrium with each other. Flow is two-dimensional and laminar while the fluid is Newtonian and incompressible. The Thermophysical properties of the Cu-H_2O nano-fluid are shown in Table. All properties are constant except the density variation is assumed that causes Buoyancy force. The Boussinesq approximation is valid as the temperature difference between wall and nano-fluid is small.

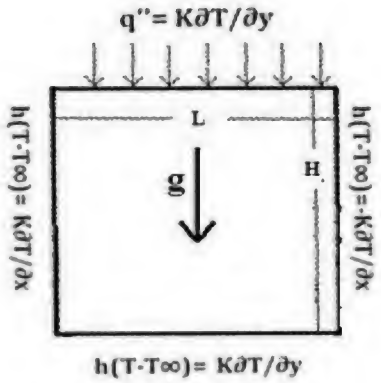

Figure 1: Schematic of Square Enclosure

Governing Equations

Governing equations shown below describes the stream-vorticity formulation of the mass, momentum and energy conservation principles and non-dimensional parameters which describe the flow and geometry along with equations that

relate velocity components and stream function.

Velocity and stream-function relationship

$$u^* = \frac{\partial \psi^*}{\partial y^*}, v^* = -\frac{\partial \psi^*}{\partial x^*}$$

Vorticity and Stream-function relationship

$$\omega^* = \frac{\partial v^*}{\partial x^*} - \frac{\partial u^*}{\partial y^*} = -\left(\frac{\partial^2 \psi^*}{\partial x^{*2}} + \frac{\partial^2 \psi^*}{\partial y^{*2}}\right)$$

Vorticity-transport equation

$$\frac{\partial \omega^*}{\partial t^*} + u^* \frac{\partial \omega^*}{\partial x^*} + v^* \frac{\partial \omega^*}{\partial y^*} = \frac{\nu_{nf}}{\nu_f} \frac{1}{\sqrt{Gr}} \left(\frac{\partial^2 \omega^*}{\partial x^{*2}} + \frac{\partial^2 \omega^*}{\partial y^{*2}}\right) + \frac{(\rho\beta)_{nf}}{\rho_{nf}\beta_f} \left(\frac{\partial \theta^*}{\partial x^*} \cos\lambda - \frac{\partial \theta^*}{\partial y^*} \sin\lambda\right)$$

Energy Equation

$$\frac{\partial \theta^*}{\partial t^*} + u^* \frac{\partial \theta^*}{\partial x^*} + v^* \frac{\partial \theta^*}{\partial y^*} = \frac{\nu_{nf}}{\nu_f} \frac{1}{Pr\sqrt{Gr}} \left(\frac{\partial^2 \theta^*}{\partial x^{*2}} + \frac{\partial^2 \theta^*}{\partial y^{*2}}\right)$$

Non-dimensional parameters

$$x^* = \frac{x}{H}, y^* = \frac{y}{H}, AR = \frac{H}{L}, \theta = \frac{T - T_\infty}{q_W^{"} H / k_f}, t^* = t\sqrt{\frac{g\beta_f q_W^{"}}{k_f}}$$

$$u^* = \frac{u}{\sqrt{\frac{g\beta_f H^2 q_W^{"}}{k_f}}}, v^* = \frac{v}{\sqrt{\frac{g\beta_f H^2 q_W^{"}}{k_f}}}, \psi^* = \frac{\psi}{\sqrt{\frac{g\beta_f H^4 q_W^{"}}{k_f}}}, \omega^* = \frac{\omega}{\sqrt{\frac{g\beta_f q_W^{"}}{k_f}}}$$

BOUNDARY CONDITIONS

Initial condition

$$at\ t^* = 0 \rightarrow u^* = 0, v^* = 0, \omega^* = 0, \psi^* = 0, \theta = 0$$

Wall boundary conditions

Heat flux boundary condition

at top wall

$$y^* = 1 \rightarrow q_W^{"} = k_f \frac{\partial T}{\partial y} \rightarrow \frac{\partial \theta}{\partial y^*} = 1$$

Convective boundary condition on other walls

at left vertical wall

$$x^* = 0 \rightarrow h(T - T_\infty) = k_f \frac{\partial \theta}{\partial x^*} \rightarrow \frac{\partial \theta}{\partial x^*} = \frac{k_{air}}{k_{nf}} Nu_{air}\theta$$

at right vertical wall

$$x^* = 1 \rightarrow h(T - T_\infty) = -k_f \frac{\partial \theta}{\partial x^*} \rightarrow \frac{\partial \theta}{\partial x^*} = -\frac{k_{air}}{k_{nf}} Nu_{air}\theta$$

at bottom wall

$$y^* = 0 \rightarrow h(T - T_\infty) = k_f \frac{\partial \theta}{\partial y^*} \rightarrow \frac{\partial \theta}{\partial y^*} = \frac{k_{air}}{k_{nf}} Nu_{air}\theta$$

NANO-FLUID PHYSICAL PROPERTIES RELATIONSHIP

Nano-fluid thermo-physical properties represent the effective thermo-physical properties of mixture of base-fluid and solid particles (nano-particles) which can alter with the solid particle volume fraction. Maxwell [19] model has been considered for effective thermal conductivity model which is valid for small particle concentration values while for effective viscosity Brinkman model [16] has been considered.

Effective Thermal Conductivity

$$k_{nf} = k_f \frac{(k_s + 2k_f) + 2\phi(k_s - k_f)}{(k_s + 2k_f) - \phi(k_s - k_f)}$$

Effective Viscosity

$$\mu_{nf} = \frac{\mu_f}{(1-\phi)^{2.5}}$$

Effective Density

$$\rho_{nf} = \rho_f(1-\phi) + \rho_s\phi$$

Effective Specific heat

$$C_{p_{nf}} = \frac{(\rho C_p)_{nf}(1-\phi) + (\rho C_p)_s\phi}{\rho_f(1-\phi) + \rho_s\phi}$$

Effective Thermal Expansion Coefficient

$$\beta_{nf} = \frac{(\rho\beta)_{nf}(1-\phi) + (\rho\beta)_s\phi}{\rho_f(1-\phi) + \rho_s\phi}$$

Table 1: Thermophysical Properties of Water and Cu-H_2O Nano-Particle

Properties	Base-Fluid (H_2O)	Nano-Particle (Cu-H_2O)
C_p (J/Kg k)	4179	383
ρ (kg/m^3)	997.1	8954
k (W/m-k)	0.613	400
β (1/k) 10^{-5}	21	1.67
α (m^2/s) 10^{-7}	1.47	1163.1

Non-Dimensional Numbers

$$Gr = \frac{g\beta_f q_w^* H^4}{k_f \nu_f^2}, Pr = \frac{\nu_f}{\alpha_f}, Nu_{air} = \frac{h_{air}H}{k_f}$$

Numerical Methodology

As for incompressible flow pressure is difficult variable to handle because there is no direct equation available for pressure calculation, stream function-vorticity approach has been adopted to solve governing equation. Finite difference technique has been used to solve coupled vorticity transport equation and energy equation in non-dimensional form. A first order forward explicit scheme has been used to discritize the temporal derivative term while convective term, diffusive term and directional temperature derivative terms have been discritized by second order central difference scheme. A non-uniform collocated grid has been used in which all the flow variables are stored at the same location.

GRID INDEPENDENCE TEST AND CODE VALIDATION

A grid independence test has been conducted for high value of Grashof number to reduce any kind of numerical error. The code has been simulated on different grid size of 11×11, 21×21, 31×31, 41×41, 51×51, 61×61, 71×71, 81×81, 91×91 and 101×101 to calculate average Nusselt number shown in Figure 3 and the result shows that an grid size of 81×81 is fair enough to describe the flow and heat transfer of the process. To check whether the code is working well or not present code has been validated with published work of De Vahl Davis [20] and Khanafer [2] et al and the results are in good match shown in Table 2.

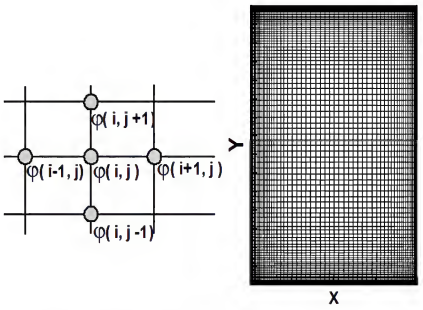

Figure 2: Collocated Grid Element and Non-Uniform Grid

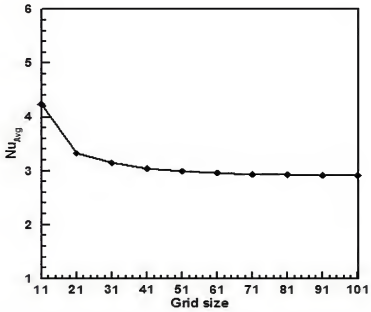

Figure 3: Grid-Independence Test for Gr=5×10^6

Table 2: Comparison of Present Results with Previous Works

Present		Khanafer et al [2]	De Vahl Davis [20]
Ra=10^4			
Nu_{avg}	2.254	2.245	2.243
u_{max} (at *y*/H)	0.193 (0.817)	0.192 (0.827)	0.192 (0.823)
v_{max}(at *x*/H)	0.235 (0.117)	0.233 (0.123)	0.234 (0.119)
Ra=10^5			
Nu_{avg}	4.614	4.522	4.519
u_{max} (at *y*/H)	0.135 (0.854)	0.131 (0.854)	0.153 (0.855)
v_{max}(at *x*/H)	0.255 (0.068)	0.258 (0.065)	0.261 (0.066)
Ra=10^6			
Nu_{avg}	8.984	8.826	8.799
u_{max} (at *y*/H)	0.080 (0.850)	0.077 (0.854)	0.079 (0.850)
v_{max}(at *x*/H)	0.258 (0.035)	0.262 (0.039)	0.262 (0.038)

RESULTS AND DISCUSSIONS

In this section the results are presented for both pure fluid and nano-fluid in square enclosure subjected to heat flux and convective boundary conditions. Considering heat flux to a constant value of 1000W/m^{2}a Grashof number has been calculated to 5×10^5. While different inclination angle has been considered to check how temperature and heat transfer

is getting affected by the different wall boundary conditions. Nano-particle concentration has been ϕ is varying up-to 4% because of limitation of the Maxwell model. Different inclination angle has been considered like 0°, 90°, 270° and 37°. These angles represents when heat flux boundary has been considered on top wall, left vertical wall, right vertical wall. While 37° inclination angle represents a specific case of Solar cell. As the boundary condition which have been considered in present study can represents a configuration of Solar cell, when sun rays are falling on the top surface of the solar cell and cell is losing heat to the surrounding by convection.

Figure 4 represents the contours of isotherms, stream lines and vorticity for different inclination angles considered for Gr = 5×10^5 and ϕ= 0. First row represents the stream-lines, second row represents the isotherms and third row represents the vorticity contours. While first, second, third and fourth column of the contours are for 0°, 90°, 270° and 37° inclination angle respectively. It can be observed from the contours that stream-line, isotherms and vorticity are very sensitive to the inclination angle. When the heat flux boundary condition has been considered at top wall which means 0° inclination angle, one can notice the counter rolling rolls of stream-lines while isotherms represent a stable temperature gradient inside the enclosure. Isotherms are seen to be almost horizontal and show conduction type of heat transfer within the enclosure. While the vortices in vorticity contours are forming in two half of the enclosure. One can notice that the stream-lines, isotherms and vorticity contours for 90° and 270° inclination angle are mirror images of each other. This can be because of the same boundary condition applied at the wall of the enclosurefor 90° and 270° inclination angle, which physically are mirror images of each other. It can be noticed that isotherms are vertical near the vertical walls of the enclosure which represents a higher temperature gradient between wall and the fluid near to it. For 37° inclination angle, it can be observed that a strong large anti-clockwise roll is formed and an additional cell is formed near the bottom corner of the enclosure due to induction by the main roll and presence of corner.

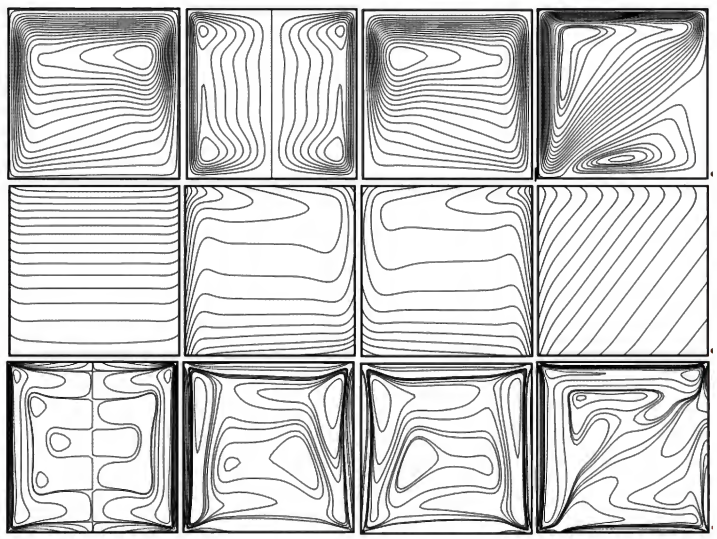

(a) (b) (c) (d)

Figure 4: Contours of Stream-Lines, Isotherms and Vorticity for Ifferent Inclination Angle λ (a) 0°, (b) 90°, (c) 270° and (d) 37°

Figure 5 represents the contours of isotherms, stream lines and vorticity for different solid nano-particle concentration values considered. First column represents the stream-lines, isotherms and vorticity contours for pure fluid (ϕ = 0%), second column is for 4% and third column is for 8% solid particle concentration. Value of ϕ has been increased up-to 8% only, because of limitation of Maxwell model. Maxwell model is a physical principal mixture rule and it is valid

for small particle concentration values only. Here results has been produced for $\lambda=90^{\circ}$ inclination angle (heat flux is at left wall). It can be observed from contours that stream-line, isotherms and vorticity are not very sensitive to particle concentration values. From stream-lines it can be observed that an egg shape central roll is forming for all concentration values and roll is on opposite side of heat flux wall that can be because of the low temperature gradient near right wall.Isotherms are vertical near heat flux wall for some distance due to higher temperature gradient while after this distance they are becoming horizontal because of the symmetric boundary condition for most of part, again they become vertical due to temperature difference between the wall and fluid near to it. While the vortices are almost same for all the particle concentration values considered. This can be because the particle concentration values which have been considered in this study are very less and because of that, changes in the effective thermal properties of the nano-fluids are almost numerically same to the base-fluid thermal properties.

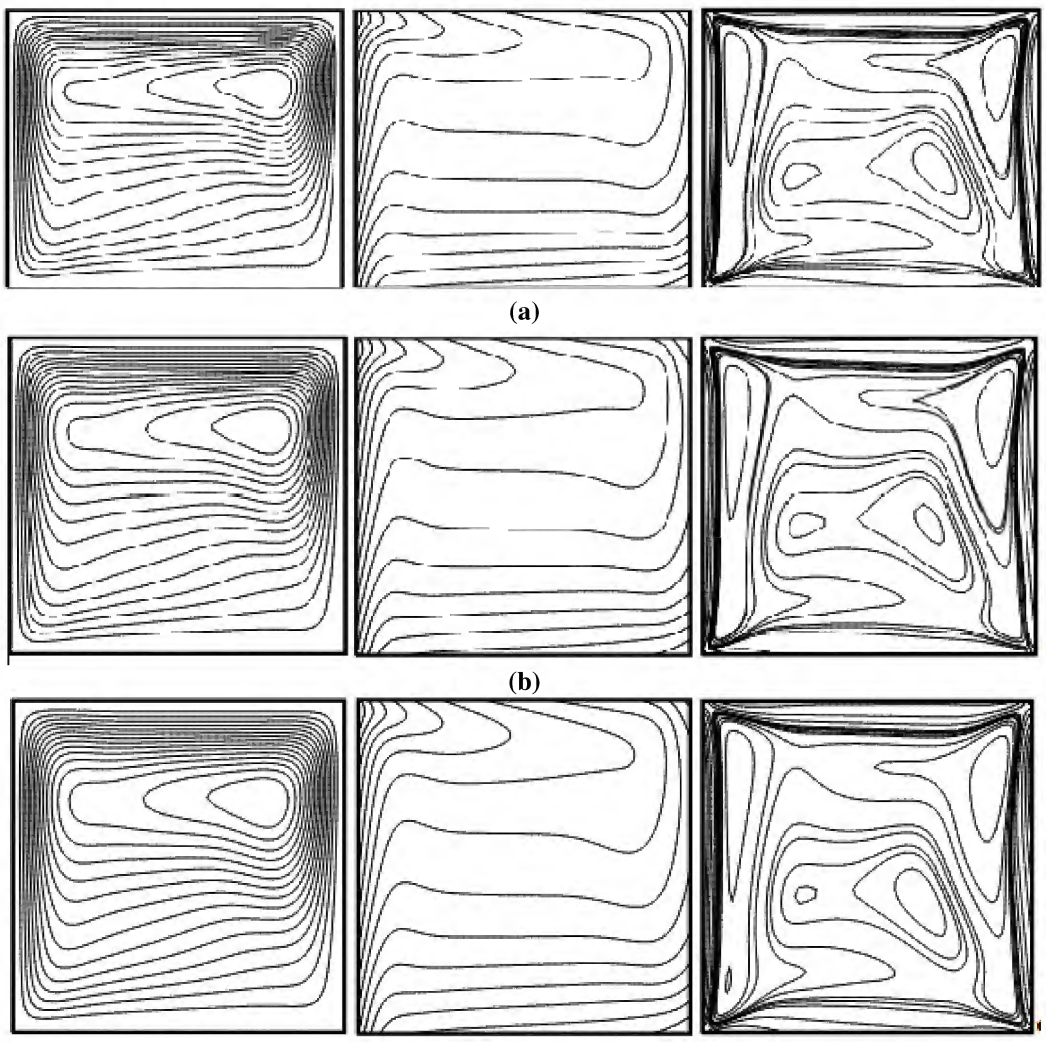

(a)

(b)

(C)

Figure 5: Contours of Stream-Lines, Isotherms and Vorticity for Different Particle Concentration ϕ (a) 0%, (b) 4% and (c) 8%

Figure 6 represents temperature profile for three different particle concentration values. Figure 6 (a) is when heat flux is acting at the left vertical wall while Figure 6 (b) is when heat flux is acting at the right vertical wall. It can be observed from figure that temperature profiles are opposite to each other in nature. This can be observed from the contours shown in Figure 4 for different inclination angle values. For 90° inclination angle (heat flux at left wall)

temperature is highest at the left vertical wall then it is decreasing because of the low temperature and then almost horizontal for most part of the enclosure and again it decreases at right vertical wall due to convective boundary condition. A vice versa nature of temperature profile for 270° inclination angle (heat flux at right wall) compared to 90° inclination angle (heat flux at left wall) can be observed because of mirror image boundary condition.

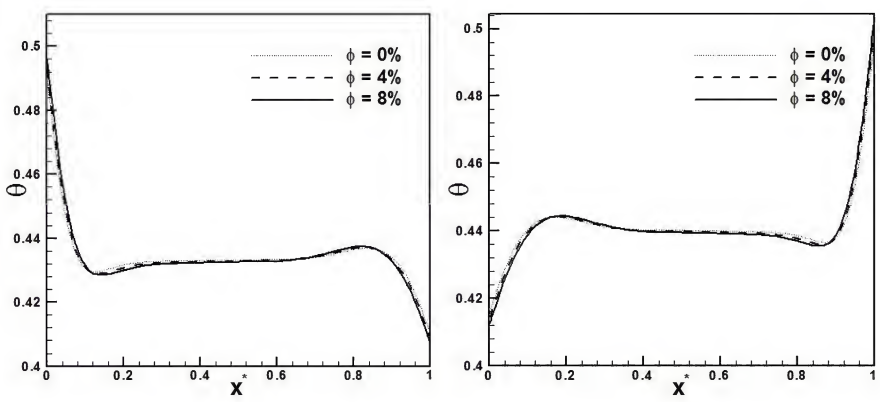

Figure 6: Temperature Profile for Different Particle Concentration Values (a) λ=90° and (b) λ=270°

Figure 7 represents vertical velocity profile for three different particle concentration values. Figure 7 (a) is when heat flux is acting at left vertical wall while Figure 7 (b) is when heat flux is acting at right vertical wall. Velocity profiles have been plotted along the horizontal plane at mid height of cavity. From figure 7(a) and 7(b) it can be observed that with an increase in nano-particle solid volume fraction, peak velocity increases, becausenanoparticles have higher effective thermal conductivity than that of base fluid (water), and they also increase the random motion and irregularity between the fluid and nanoparticle. Addition of nanometric-size particles in base fluid also increases the surface area volume ratio, which indirectly will give more surface area for reaction to take place and the energy exchange to occur at higher rates. The resultant effect eventually increases the overall heat-transfer rate and velocities peaks. Figure 7(a) and 7(b) are mirror image of each other the reason is same as explained earlier in the text.

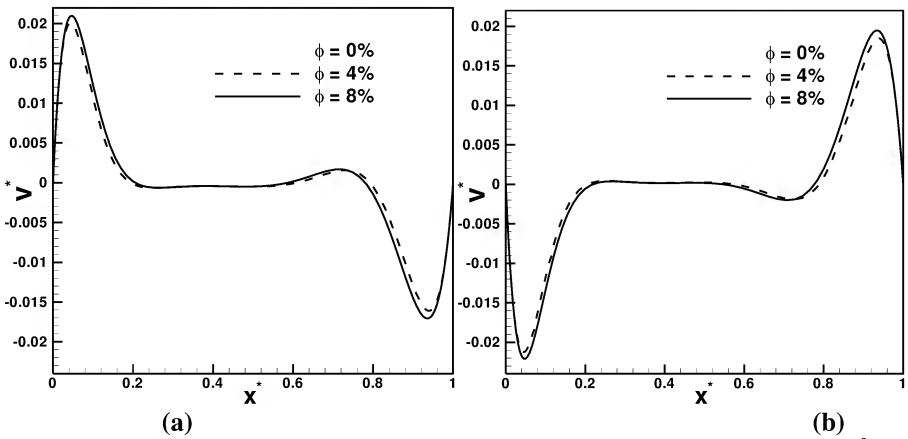

Figure 7: Vertical Velocity Profile for Different Particle Concentration Values (a) λ=90° and (b) λ=270°

Figure 8 represents the temperature profiles for different inclination angle values 0°, 90° and 37°. Figure 8 (a) is for pure fluid case ϕ=0 while Figure 8 (b) is for Cu-H_2O nano-fluid for three different solid particle concentration values. These temperature profiles have been plotted perpendicular to the heat flux boundary wall. It can be observed from figure 8 (a) that at 0° inclination angle (Heat Flux at the top wall) maximum temperature has been found then it is decreasing continuously because from all other three walls heat is losing to the surrounding by convection.

While a minimum temperature has been found for 90° inclination angle (Heat Flux at the left wall) compared to that of 0° (Heat Flux at the top wall) inclination angle, because at 0° inclination angle heat flux is incident directly at the wall. Addition of nano-particle in the base-fluid is not showing any significant changes in the temperature profiles all the curves are following the same path.

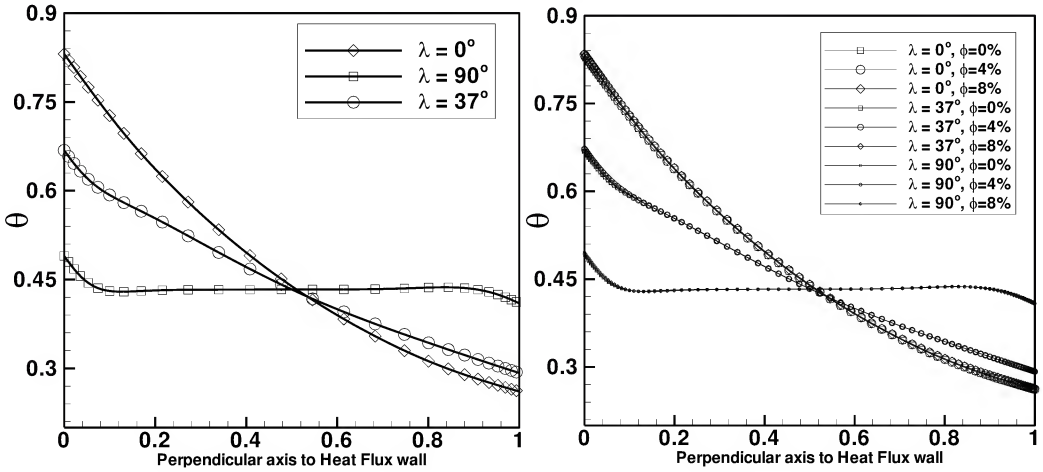

Figure 8: Temperature Profile for Different λ Values (a) For Pure-Fluid (b) With Particle Concentration

Figure 9 (a-b) represents the variation of Nusselt number at the left vertical wall for different inclination angles. Effect of solid particle concentration has also been included. Figure a and b are for 37° and 233° inclination angles while figure c and d are for 90° and 270° inclination angles. Definition of Nusselt number has been adopted from Alloui et al [10].

$$Nu = \frac{hH}{k_{nf}} = \frac{q_w^{"}}{\Delta T}\frac{H}{k_{nf}} = \frac{k_f}{k_{nf}}\frac{1}{\theta_w - \theta_c}$$

It can be observed that for 37° inclination angles Nuseelt number is decreasing continuously along the length of the wall, this can be because as the centre point temperature of the enclosure is constant and the temperature of the wall is increasing with the height so the difference is also increasing which decreasing the Nusselt number at the wall, but at the top of the wall Nusselt number is again increasing because temperature is again decreasing at the top of the wall which one can observe from the contours of the isotherms. Figure (a) and (b) are mirror image of each other; reason is same as explained earlier in the text. One can observe from Figure (c) That Nusselt number in initially increasing than it is decreasing because initially the temperature at the wall is decreasing which one can observe from the temperature profiles in Figure 6. Figure (c) and (d) are mirror image of each other because of the mirror image boundary condition. Increase in the particle concentration values is decreasing the Nusselt number, decrease for 37°and 233° inclination angle is numerically less compare to 90° and 270° inclination angles.

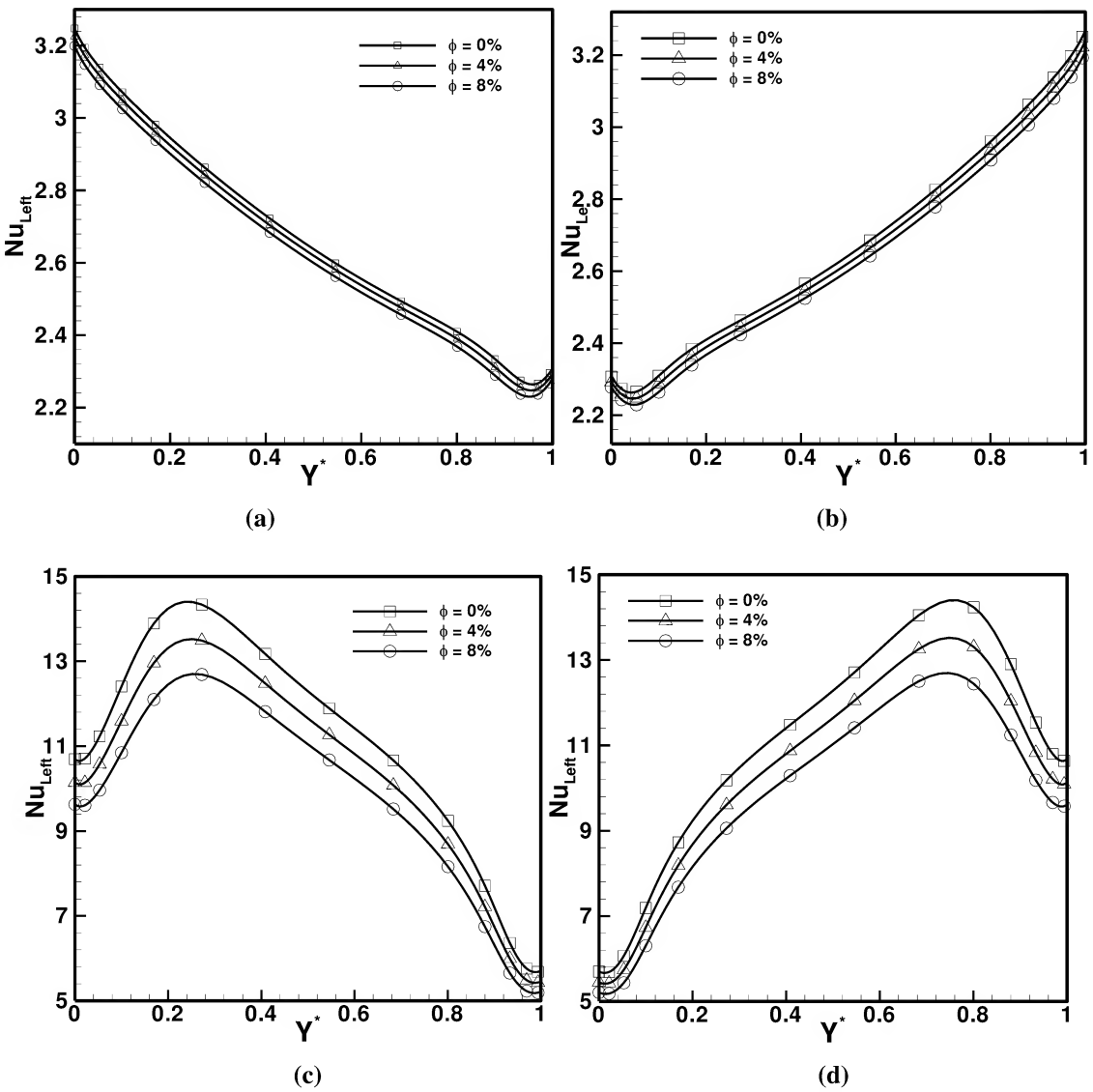

Figure 9: Nusselt Number for Different λ Values (a) 37° (b) 233° (c) 90° (d) 270°

CONCLUSIONS

Natural convection in a square enclosure filled with Cu-H_2O nanofluid has been examined with convective and heat flux boundary condition. Heat flux boundary condition has been considered only at the one wall while on other three walls convective boundary condition has been considered. Basic aim of the present study is to see the effect of heat flux boundary and convective boundary on the heat transfer rate and flow patterns. Results have been produced for different inclination angle of the enclosure. Grashof number in the study has been kept constant to 5×10^5 based on the heat flux value considered while Prandtl number Pr = 6.49 have been used for water.

Results found in the study are as follows,

- Flow is very sensitive to the inclination angle or heat flux boundary. When the heat flux boundary is at the top wall means 0° inclination angle, counter rolling rolls of stream-lines has been observed while isotherms represent a stable temperature gradient inside the enclosure.

- Stream-lines, isotherms and vorticity contours for 90° and 270° inclination angle are mirror images of each other. This is because of the boundary condition applied at the wall of the enclosurefor 90° and 270° inclination angle, which physically are mirror images of each other.
- For 37° inclination angle a strong large anti-clockwise roll and an additional cell is formed near the bottom corner of the enclosure due to induction by the main roll and presence of corner.
- Addition of nano-fluid is not showing any relevant changes in the flow pattern. An egg shape central roll is forming for all the concentration values and the roll is on opposite side of the heat flux wall that can be because of the low temperature gradient near the right vertical wall.
- Nusselt number for 37° inclination angle is decreasing with the height while for 90° inclination angle first it is increasing then it decreases throughout the height of the enclosure.
- Nusselt number is decreasing with the addition of nano-particle in the base-fluid for all ϕ values.

ACKNOWLEDGEMENTS

I would like to thank to my supervisor Dr. Arun K. Saha for his neat and kind support without whom this work would not have been completed. I would also like to express my sincere thanks to Dr. Malay K. Das. Regular meetings and asking about work progress by Dr. Arun K. Saha and Dr. Malay. K Das have helped me in better understanding of the problem and in successful completion of this work. I would like to thank to the teachers of Mechanical department of IIT Kanpur whose generous support in courses has helped me vastly throughout the research period.

REFERENCES

1. Kakac, S. & Pramuanjaroenkij, A. (2009), Review of convective heat transfer enhancement with nanofluids, *International Journal of Heat and Mass Transfer*, 52, pp.3187-3196.
2. Khanafer, K. & Vafai, L. & Lightstone, M. (2003), Buoyancy-driven heat transfer enhancement in a two-dimensional enclosure utilizing nanofluids, *International Journal of Heat and Mass Transfer,* 46, pp.3639-3653.
3. Abu-Nada, E. & Oztop, H.F. (2009), Effects of inclination angle on natural convection in enclosures filled with Cu–water nanofluid, *International Journal of Heat and Fluid Flow,*30,pp.669-678.
4. Rubel, A. & Landis, F. (1969), Numerical study of natural convection in a vertical rectangular enclosure, *Physics of Fluids,* 12,II-pp.208-213.
5. Ozoe, H. & Sayama, H. & Churchill, S.W. (1974),Natural convection in an inclined square channel, *International Journal of Heat and Mass Transfer*, 17, pp.401-406.
6. Ghasemi, B. & Aminossadati, S.M. (2009), Natural convection heat transfer in an inclined enclosure filled with a water-cuo nanofluid, *Numerical Heat Transfer, Part A,* 55, pp.807-823.
7. Ogut, E.B. (2009), Natural convection of water-based nanofluids in an inclined enclosure with a heat source, *International Journal of Thermal Sciences,* 48, pp.2063-2073.

8. Santra, A. K. & Sen, S. & Chkraborty. (2008), Study of heat transfer augmentation in a differentially heated square cavity using copper–water nanofluid, *International Journal of Thermal Sciences,* 47, pp.1113-1122.

9. Jou, R.-Y. & Tzeng, S.-C. (2006), Numerical research of nature convective heat transfer enhancement filled with nanofluids in rectangular enclosures, *International Communications in Heat and Mass Transfer,* 33, pp.727-736.

10. Alloui, Z. & Vasseur, P. & Reggio, M. (2012), Analytical and numerical study of buoyancy-driven convection in a vertical enclosure filled with nanofluids, *Heat and Mass Transfer,* 48, pp.627-639.

11. Tiwari, R.K. & Das, M.K. (2007), Heat transfer augmentation in a two-sided lid-driven differentially heated square cavity utilizing nanofluids, *International Journal of Heat and Mass Transfer*50, pp.2002-2018.

12. Talebi, F. & Mahmoudi, A. H. & Shahi, M. (2010), Numerical study of mixed convection flows in a square lid-driven cavity utilizing nanofluid, *International Communications in Heat and Mass Transfer,* 37,pp.79-90.

13. Khanafer, K.M. & Al-Amiri, A. M. & Pop, I. (2007), Numerical simulation of unsteady mixed convection in a driven cavity using an externally excited sliding lid, *European Journal of Mechanics B/Fluids,* 26, pp.669-687.

14. Jang, S.P. & Choi, S.U.S. (2004), Role of Brownian motion in the enhanced thermal conductivity of nano-fluids, *Applied Physics Letters,* 84, pp.4316-4318.

15. Azizian, M.R. & Aybar, H.S. & Okutucu, T. (2009), Effect of Nanoconvection due to Brownian motion on Thermal Conductivity of nanofluids, *Proceedings of the 7th IASME /WSEAS International Conference on HEAT TRANSFER, THERMAL ENGINEERING and ENVIRONMENT* pp.53-56.

16. Brinkman, H. C. (1952), The Viscosity of Concentrated Suspensions and Solutions, *The Journal of Chemical Physics,* 20,pp.571

17. Murshed, S.M.S. & De Castro, C.A.N. (2011), Contribution of Brownian motion in Thermal Conductivity of Nanofluids, *Proceedings of the World Congress on Engineering.*

18. Singh, A. K. (2008), Thermal Conductivity of Nanofluids, *Defence Science Journal, 58,* pp.600-607.

19. J. Clerk Maxwell, (1892),"A Treatise on Electricity and Magnetism", 3rd ed., vol. 2. Oxford: Clarendon, pp.68–73.

20. G. De, Vahl Davis, (1962), Natural convection of air in a square cavity, a benchmark numerical solution, *International Journal for Numerical Methods in Fluids,* 3, pp.249–264.

21. Kosti, S. &Das, M. K. & Saha A. K.. (2013), Buoyancy-driven flow and heat transfer in a nano-fluid-filled enclosure, *Nanomaterials and Energy*, 2(4), 200-211.